



# Microfluidic technology for cell biology–related applications: a review

Joydeb Mukherjee<sup>1</sup> · Deepa Chaturvedi<sup>2</sup> · Shlok Mishra<sup>3</sup> · Ratnesh Jain<sup>1</sup> · Prajakta Dandekar<sup>2</sup>

Received: 12 June 2023 / Accepted: 13 November 2023 / Published online: 6 December 2023  
© The Author(s), under exclusive licence to Springer Nature B.V. 2023

## Abstract

Fluid flow at the microscale level exhibits a unique phenomenon that can be explored to fabricate microfluidic devices integrated with components that can perform various biological functions. In this manuscript, the importance of physics for microscale fluid dynamics using microfluidic devices has been reviewed. Microfluidic devices provide new opportunities with regard to spatial and temporal control over cell growth. Furthermore, the manuscript presents an overview of cellular stimuli observed by combining surfaces that mimic the complex biochemistries and different geometries of the extracellular matrix, with microfluidic channels regulating the transport of fluids, soluble factors, etc. We have also explained the concept of mechanotransduction, which defines the relation between mechanical force and biological response. Furthermore, the manipulation of cellular microenvironments by the use of microfluidic systems has been highlighted as a useful device for basic cell biology research activities. Finally, the article focuses on highly integrated microfluidic platforms that exhibit immense potential for biomedical and pharmaceutical research as robust and portable point-of-care diagnostic devices for the assessment of clinical samples.

**Keywords** Cell biology · Microfluidics · Cell stimulation · Cancer cell · Cell sorting

## 1 Introduction

An innovative approach in cell biology, the ability of microfluidic devices to deliver chemical cues with spatial precision comparable to the sub-cellular dimensions, can resolve biological issues at the level of individual cells. In microfluidic technology, we can expose the cells to gradient streams of chemicals, like hormones, cytokines, growth factors,

---

✉ Prajakta Dandekar  
pd.jain@ictmumbai.edu.in

<sup>1</sup> Department of Biological Science and Biotechnology, Institute of Chemical Technology, Mumbai 400019, India

<sup>2</sup> Department of Pharmaceutical Sciences and Technology, Institute of Chemical Technology, Mumbai 400019, India

<sup>3</sup> Department of Chemical Engineering, Institute of Chemical Technology, Mumbai 400019, India

and chemoattractants. Furthermore, we are able to assess each cell's unique reaction to mechanical stimulation. As the cell physiology, phenotype, and functionality are governed by the physicochemical operating conditions of the neighboring cells, microfluidic devices present a novel way to determine cellular fate during *in vitro* investigations. The motivation for integrating several time-consuming steps into solitary monolithic micro-platforms was considered the initial impetus for fabricating microfluidic systems for cell culture applications [1]. Again, the majority of the microfluidic systems for cell culture applications can be simply defined as the miniaturized versions of conventional lab-scale processes. These are based on the requirement of low sample volumes, and they are easy to fabricate and are compatible with most biological assays [2]. In other words, microfluidic devices can be designed to explore the previously unknown aspects of cell biology.

The creation of microfluidic cell culture systems was spurred by the difficulty of macroscale culture techniques to recapitulate interactions between the cells, the analytes, and the extracellular matrix (ECM). In the past few years, biophysical and biochemical insights into cells and tissues have been obtained by the combination of cell culture with microfluidic devices. In addition, cell-based sensors are being employed for biochemical, biomedical, and environmental applications. Most of the microscale applications depend upon short-term responses due to cell–cell interactions within the microdomain. Several essential cellular processes occur over longer time scales [3]. To understand the cell–cell interaction, cell differentiation, and proliferation of cells within the microfluidic devices, microfluidic platforms can also be developed to mimic cellular homeostasis [4]. Accordingly, long-term cell culture platforms have been developed to expose the cells to a gradient of analyte concentrations [5]. Typically, cells are restricted to specific regions of the microchannel devices, which can also be created by micropatterning of cells. This concept can promote cell adhesion or can be used to generate hydrodynamic cell trap arrays or dielectrophoretic trap arrays [6]. Through this manuscript, we have presented a comprehensive overview of the application of microfluidic technology in the biomolecular and biomedical fields. We have also included several significant examples of the use of microfluidic technology in cell biology, along with a brief overview of the fundamental physics underlying this technology.

## 2 Microscale flow physics for biological application

Fluid flow at the microscale level is a unique phenomenon that can be used to fabricate small-scale microfluidic devices and components that can perform different biological functions. The other review articles related to microfluidic systems have already focused on the physics of the microscale phenomena and how it can be useful to fabricate certain microdevices [1–4]. Hence, in this article, the importance of microscale flow physics has been reviewed for a deeper understanding of the microscale biological applications.

Microfluidic technology handles and analyzes fluids within the miniaturized systems, where the length scale of the devices lies in the microscale range. At this range, the different forces formed due to downscaling and shrinkage of large conventional devices become dominant over those experienced in everyday life [5]. Thus, new device designs involving microscale flow physics have been employed to understand the different applied forces at the microscale level. The physical effects that are dominant in microfluidic devices include the laminar flow, fluidic diffusion resistance, surface area-to-volume ratio, and surface tension. An excellent review presenting an overview of the microscale flow physics at the nanoliter scale has been published earlier [6].

## 2.1 Dimensionless numbers

In classical fluid mechanics, flow physics is described in terms of important dimensionless numbers that define the interplay between the different applied forces within the microscale flow domain. In the case of fluid mechanics and species transport, the two most celebrated non-dimensional numbers that describe the microscale flow phenomenon include the Reynolds number (Re), which considers the ratios between the inertial and viscous forces, and the solute Peclet number that defines the ratio between convective and diffusive forces, respectively. Values of these dimensionless numbers are significantly different when the length scale of the devices is reduced from macro- to microscale.

In the case of the forced flows within the microfluidic device, the Re is the most important dimensionless number that characterizes the flow regimes, i.e., the laminar and turbulent, respectively. In the laminar flow, the velocity of the fluid particle elements in the fluid stream is not defined in terms of random motion as a function of the time scale. In other words, the turbulent flow is chaotic and unpredictable, which means that it is impossible to predict the position of the fluid particle elements in the fluid streams as a function of time. So, the most celebrated non-dimensional number in microscale flow physics, the Reynolds number, is defined as stated in Eq. (1):

$$\text{Re} = \frac{\rho v D_h}{\mu} \quad (1)$$

where  $\rho$  is the density of the working fluid system,  $v$  is the characteristic velocity of the fluid streams,  $\mu$  is the dynamic viscosity of the fluid systems, and  $D_h$  is the hydraulic diameter, respectively. The hydraulic diameter depends on the cross-sectional area of the proposed microfluidic geometry.  $\text{Re} < 2300$ , as calculated by using Eq. (1), indicates the laminar flow behavior of the fluid streams. In the context of the turbulent flow behavior, the operating Reynolds number, Re, is greater than 2300. The existing literature reports reveal that Re for transition flows (laminar to turbulent) within the microfluidic channels may be different as compared to the theoretical predictions.

The flow velocity within the microfluidic devices generally varies within 1  $\mu\text{m/s}$  to 1 cm/s, wherein the hydraulic diameter,  $D_h$ , is 10  $\mu\text{m}$ , and the Re is in the range of  $10^{-6}$  to  $10^1$ . In this operating Re, the non-linearity term is mostly neglected in the presence of the inertia effects, and turbulence behavior is unlikely. Based on previous reports, the value of the critical Re in the transition regime (from laminar to turbulent flow) is lower as compared to the critical Re for the macroscale flow behavior [7]. Thus, to understand these effects related to the critical Re, based on the transition flow regime behavior, investigations have been conducted to study the effects imparted by the surface features. In other words, flow friction, which is defined in terms of fluidic resistance, has emerged as a major factor in understanding microscale flow physics [8].

Owing to the low Re hydrodynamics in the microfluidic domain, mixing within the microchannel devices is hindered. Additionally, in the macroscale flow physics behavior, the origin of mixing can be traced in terms of the chaotic eddies, which are formed under the influence of turbulence. Thus, mixing due to diffusion phenomena can be realized within the microchannels. Hence, depending upon the targeted application, diffusive mixing can either be advantageous for the reaction within the microchannels or ineffective for particle separation. In order to understand the diffusive mixing process, it is imperative to explain another important non-dimensional number, the Peclet number. By definition, the Peclet number is defined in terms of the relative strength of convection over diffusion and is defined in Eq. (2):

$$Pe = \frac{vw}{D} \quad (2)$$

where  $w$  is the width of the proposed microchannel system and  $D$  is the diffusivity coefficient of the solute particles. In the context of the biological systems, the diffusivity,  $D$ , is in the range of  $10^{-10}$  ( $\text{m}^2/\text{s}$ ), the width of the microchannel is  $10 \mu\text{m}$ , velocity  $v$  is approximately  $1 \text{ m/s}$ , and it takes approximately 100-microchannel width to complete the diffusive mixing process. In the case of a lower strength of the diffusion phenomenon, different innovative strategies for mixing, under the influence of the secondary or transverse flows, have already been invented [9]. In the microscale flow phenomenon, diffusion times can be short, and microchannels are used to develop the concentration gradients with nonlinear profiles [10, 11]. Mixing schemes between the two fluid streams at the microscopic level must be improved to maximize the interfaces between the two fluid streams and to allow the diffusion process to occur quickly [12, 13].

Considering the theoretical predictions performed by several authors, Ajdari et al. studied structured chaotic micromixing devices to understand the concentration distribution between two fluid streams. Indeed, there are multiple occasions where the mechanisms of active and passive micromixing processes have been used to develop micromixers. Active micromixers are based on the geometrical features of microchannel devices. Passive micromixing processes that use passive micromixers include Taylor dispersion analysis, hydrodynamic focusing, split and recombine flows, chaotic advection, and electrokinetic instability [14–18]. In other words, active micromixing includes rotational micromixing, dielectrophoresis, AC electrokinetic instability, fluid-induced electroosmosis, and electro-wetting on dielectric, respectively [19–23]. However, researchers are trying to develop an optimum strategy for mixing within the microchannel devices.

Other important non-dimensional numbers related to microscale flow physics include the Knudsen number,  $Kn$ , defined in terms of the ratio between mean free path with the characteristics length of the proposed system; the Weissenberg number,  $Wi$ , which is the ratio between the relaxation time and shear rate of the polymeric molecules; the capillary number,  $Ca$ , which is the ratio of the viscous force to surface tension force; and the Deborah number,  $De$ , which is the ratio between the polymer relaxation time and characteristic flow time.

In this study, we consider several non-dimensional numbers (as mentioned in Table 1) which have depicted the positive effect on performance of a system in terms of scale-up study. This involves increased throughput and mass parallelization of on-chip processes [24]. In order to address several issues, including designs for biocompatibility, efficiency, and cost-effectiveness of microfluidic devices, increased awareness of the biological processes by engineers, and methods for standardization and system integration of modular components, a collaborative effort involving physicians, scientists, and engineers is required.

## 2.2 Physicochemical properties of biofluids

The viscosity of the fluid is defined in terms of the resistance of the fluid motion and can be measured by relating shear force and velocity gradients or the strain rate in a flowing fluid, as explained by Newton's law of viscosity stated in Eq. (3):

$$\tau = -\mu\dot{\gamma} \quad (3)$$

where  $\tau$  is the force per unit area,  $\dot{\gamma}$  is the shear rate, and  $\mu$  is the dynamic viscosity of the working fluid system, respectively.

**Table 1** Non-dimensional numbers commonly used in the analysis of microfluidic systems for cell biology applications [24]

Non-dimensional numbers	Notation	Ratio
Reynolds number	Re	Inertia force/viscous force
Peclet number	Pe	Convection/diffusion
Weissenberg number	Wi	Shear rate $\times$ relaxation time
Deborah number	De	Relaxation time/flow time
Dean number	Dn	Transverse flow/longitudinal flow
Capillary number	Ca	Viscous/interfacial
Weber number	We	Inertial/surface tension
Stokes number	$N_{st}$	Viscous force/gravitational force

The shear rate and shear stress ratio of biological fluids, which are categorized as pseudoplastic non-Newtonian fluid systems, affect the fluid's viscosity. The power law obeying model is used to characterize these events [14], as defined in Eq. (4).

$$\tau = K(\dot{\gamma})^{n-1} \quad (4)$$

where  $K$  is the consistency index and  $n$  is the flow behavior index.

The above-mentioned parameters are used to characterize the rheological behavior of power law obeying fluids. For the value of  $n$  equal to 1, the behavior of the fluid is of Newtonian type;  $n > 1$  is for the dilatants, and  $n < 1$  is associated to the pseudoplastic fluid behavior with an apparent viscosity ( $\mu_a$ ) that increases or decreases, respectively, with an increase in the shear rate.

Fahraeus and Lindqvist were the pioneers in exhibiting the dependence of relative apparent viscosity and hematocrit ( $\sim 40\%$  v/v) on the radius of the tube. Additionally, Zharov et al. [16] studied the flow behavior of RBCs using micropillars, which indicated the physicochemical properties, including the velocity and thickness of the suspending medium separating the tube wall from the cell. This process depends on pressure drop, the diameter of capillary, and volume fraction of RBCs as well as the RBC's shape deformation in flow.

Media solution bathing cells consist of ions, carbohydrates, gases, and proteins, which increase fluid viscosities and conductivities. In experiments using microfluidic systems to manipulate cells, an ideal suspension mixture is often avoided in favor of Newtonian solutions with low viscosity, that is, water-based solutions, to ensure that the resistance to the fluid flow and saturation of the technological limits are minimized. As microfluidic networks and on-chip mixing and dilution of fluids become more complicated and changes in hydrodynamic resistance due to viscosity changes, manifest, microfluidic geometries, interfaces, and integrated components must be taken into consideration from the very start of the design process [17].

## 2.3 Hydrodynamics in microchannels

Conventional methods for flow actuation mechanisms within microfluidic systems are pressure driven or electrokinetically driven [18, 19]. For an incompressible fluid, where density does not change as a function of time, the equivalent of Newton's second law motion (i.e.,

$F = ma$ ,  $m =$  mass of the object,  $a =$  acceleration of the objects) can be defined in terms of the Navier–Stokes equation, as expressed in Eq. (5).

$$-\nabla P + \mu \nabla^2 \mathbf{u} + \mathbf{F}_b = \rho \frac{\partial \mathbf{u}}{\partial t} + \rho \mathbf{u} \cdot \nabla \mathbf{u} \quad (5)$$

where  $\mathbf{u}$  is the velocity field ( $\text{m}\cdot\text{s}^{-1}$ ),  $P$  is the acting fluid pressure (Pa), and  $\mathbf{F}_b$  is the external body forces acting on the bulk liquid per unit volume i.e., magnetic and electrical potential, etc.

Microflows predominantly fall under the category of the laminar region ( $\text{Re} < 1$ , creeping flow behavior is followed up). Thus, the Navier–Stokes equation can be converted into the Stokes equation by ignoring the nonlinear convective factor in Eq. (5) and the external body forces to predict the linear flow in a microchannel [20]. Here, Stokes equation is defined in Eq. (6), which becomes

$$\rho \frac{\partial \mathbf{u}}{\partial t} = -\nabla P + \mu \nabla^2 \mathbf{u} \quad (6)$$

Using the mass continuity equation to calculate the fluid flow of an incompressible fluid, i.e.,  $\nabla \cdot \mathbf{u} = 0$ , we get a linear expression to determine the pressure drop at low operating Reynolds number, with variation in pressure in the axial direction of the microchannel. So, Eq. (6) can be rewritten as follows:

$$\mu \nabla^2 \mathbf{u} = \frac{dP}{dX} \quad (7)$$

In Eq. (7), we consider the steady-state flow behavior which is away from the entrance of the microchannel system and axial direction of the channel height, where the height of the microchannel,  $h$ , is much less as compared to the width ( $w$ ) and length ( $L$ ) of the microchannel system (i.e.,  $h \ll w$  and  $L$ ) [24].

Now, to solve Eq. (7), we apply no-slip boundary conditions (i.e.,  $u = 0$ ) and obtain the resulting equation, as stated in Eq. (8), to understand the Poiseuille profile flow.

$$u = -\frac{dP}{dx} \frac{h^2}{2\mu} \left( 1 - \frac{y^2}{h^2} \right) \quad (8)$$

For circular microchannel systems, the average velocity is obtained as  $u_{\text{avg}} = \frac{Q}{A}$ , where  $Q$  is the volumetric flow rate ( $\text{m}^3\cdot\text{s}^{-1}$ ) and  $A$  is the cross-sectional area of the channel ( $\text{m}^2$ ). Considering no-slip boundary condition at the wall of the tube, i.e.,  $r = 0$  and  $u = 0$ , for fully developed laminar parabolic flow, maximum velocity is obtained at the centerline of the microchannel system and the volumetric flow rate is defined as stated in Eq. (9).

$$Q = \frac{1}{2} u_{\text{max}} \pi R^2 = \frac{\pi R^4}{8\mu} \left[ -\frac{d}{dx} (P + \rho g z) \right] \quad (9)$$

Equation (9) explains the Hagen–Poiseuille flow, considering the fluid’s resistance to evaluate the pressure drop in circular channels (as stated in Eq. (10)), assuming  $z = 0$ , i.e., horizontal microchannel:

$$\Delta P = \frac{8\mu L Q}{\pi R^4} = QR_H \quad (10)$$

Rectangular microchannel systems, with aspect ratios  $\alpha = \frac{w}{h}$ , where the microchannel width ( $w$ ) is greater as compared to the height of the microchannel ( $h$ ) or  $w > h$ , have flows that are characteristic of Hale-Shaw flow, as defined in Eq. (10). The flow profile remains parabolic along with the height of the microchannel system, but as the aspect ratio increases, the average velocity across the width of the microchannel system becomes increasingly plug-like, which is presented in Eq. (11).

$$\Delta P = \frac{12\mu LQ}{\pi R^4} = QR_H \quad (11)$$

In case where  $w < h$ , Eq. (11) is changed to Eq. (12), providing a less than 0.3% error for aspect ratio,  $\alpha < 1$  and Reynolds number is less than 1000 [21–23]:

$$P = \frac{12\mu LQ}{wh^3} \left[ 1 - \frac{0.63h}{w} \tanh\left(\frac{\pi w}{2h}\right) \right]^{-1} \quad (12)$$

If  $\alpha = 1$ , the maximum flow for a given pressure differential will exist for a given cross-sectional area and can be estimated as follows:

$$\Delta P = \frac{32\mu LQ}{h^4} \quad (13)$$

From Eqs. (10)–(13), we can observe that the pressure drops within the microchannel are affected by the volumetric flow rate and the resistance of the fluid to the flow, the values determined by the geometry of the microchannel.

### 3 Cell biology: microfluidics

Cellular processes in cell adhesion, cell migration, cell growth, etc., are controlled and influenced by their three-dimensional biomolecular organization, which is generally difficult to be reproduced in the laboratory. Furthermore, the cells respond to local concentrations of a variety of biomolecules, such as enzymes, nutrients, and small ions that may be dissolved in the extracellular medium or present on the extracellular matrix protein surfaces or the surface adjacent to the cells, i.e., membrane receptors [25]. In the context of the traditional cell culture system, these factors are homogeneously distributed over the substrate on which the cells grow. To understand the behavior of cells in culture, it is necessary to focus on the cell patterning method, such that it promotes selective cell attachment like a thin adhesive template and provides the physical barrier that can be used to remove the cells without inflicting any damage to them [26]. In this section we will provide an explanation of the three aspects in terms of mechanobiology concept in which we explain the relationship between the mechanical response and the biological response of cells under the physiological shear stress and the application of microfluidic device in the cell biology-related applications i.e., cell-based assays carried out in microfluidic devices, and microfabricated cell culture systems, which covers various in vitro studies related to the influence of the microenvironment on cell integrity.

### 3.1 Microfabricated cell culture systems

Culturing cells *in vitro* is one of the foundations of modern biology. Nevertheless, many essential factors have to be taken into consideration, which makes it difficult to mimic natural tissues under *in vitro* conditions [27]. The microfluidic platforms are used to increase the control over cell–cell interactions and the soluble cues in the natural cellular environment. In the context of cell biology application within the microfluidic device, microfluidic devices offer an additional advantage of being capable of creating mechanical strain, under the influence of shear, in the physiological range.

### 3.2 Cells and extracellular matrix

Advanced surface chemistry makes it possible to reproduce and engineer cell microenvironments, at cellular resolution, by micropatterning techniques. A large variety of surface patterning techniques are employed for microfluidic devices, including the standard lithography or the liftoff technique, photoreactive chemistry, and soft lithography technique, based on microcontact printing and fluidic printing [28]. The surface patterning technique is used to develop micrometer-sized features. Also, this technique is used to control cell–extracellular matrix interactions and for the creation of cell ensembles of specific geometry. Lamination and photopolymerization methods have also been used to develop three-dimensional (3D) scaffolds in the micrometer range, using biodegradable materials. These 3D scaffolds also mimic the extracellular matrix (ECM), a dynamic network present in all tissues and organs that not only provides mechanical support but also guides cell behavior, functions, and tissue features. Although the relevance of the ECM is widely understood, integration of well-controlled ECMs into organ-on-chips (OoCs), developed using microfluidic devices, still remains a challenge. Hence, methods for modulating and assessing the ECM features within the OoCs are still under development. Development of these methods will help us to understand the properties of ECM and ECM-like materials, as shown in Fig. 1a, b. This may enable the accurate operation and control of microfluidic devices used in OoC platforms and ultimately may facilitate realistic elucidation of the biochemical and mechanical processes responsible for cell behavior.

It is possible to estimate mechanical forces on ECM by cells in various ways. A specific and effective technique to measure the deflection of the arrays is with the help of micrometer-sized vertical elastomer posts. In the case of the smooth muscle cells, the applied forces act on the substrate plane in the order of 100 nN and appear to the scale of the area covered by the focal adhesions [30]. When compared to the conventional methods that depend on substrate deformation, the elastomer post approach offers greater precision and adaptability: without altering surface chemistry, post-geometries can change a surface's mechanical properties [30].

#### 3.2.1 Microenvironment on cell integrity

In order to promote meaningful research about cell-based processes, cells must be able to sustain their *in vitro* activity. To create systems that might promote the survival of the cell for a longer duration, one needs a comprehensive knowledge of cell characteristics and elements that might lead to cellular damage in microfluidic systems. In terms of



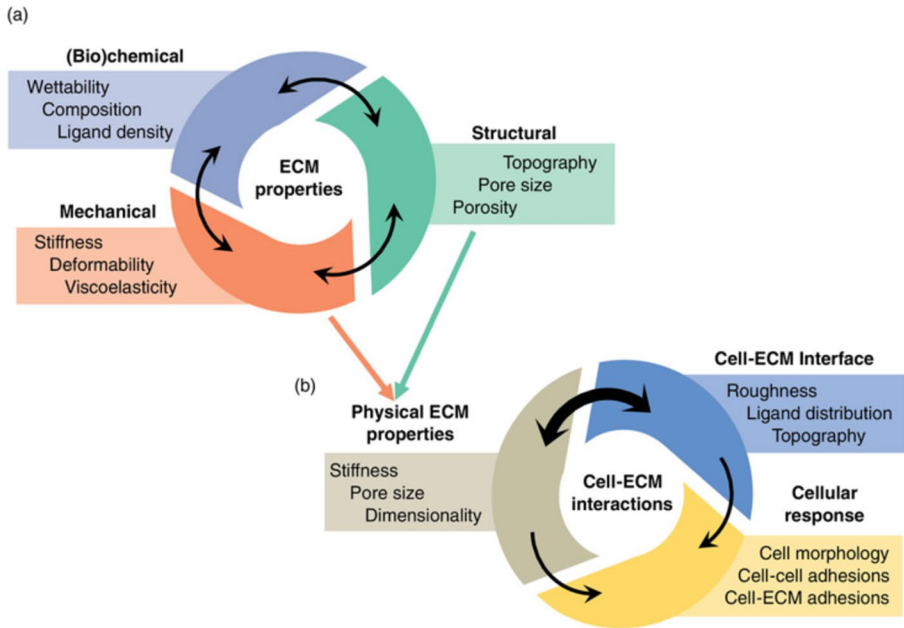


**Fig. 1** **a** Relationship between ECM material characteristics and **b** interrelation between cells and ECM and how they affect cellular responses (adapted from [29], with permission from Wiley)

their structures and functions, cells are classified into prokaryotic or eukaryotic cells [31]. They are made up structurally of a fluid-filled interior space called the cytoplasm, which houses microscopic organelles such as the cytoskeleton, mitochondria, and ribosomes. These organelles play a variety of roles in maintaining the internal and external microenvironments during a variety of biological processes like cellular respiration, DNA replication, biochemical signaling, and protein synthesis. A semi-permeable membrane that encloses the cytoplasm is mainly made up of two phospholipids that are next to one another, and each has a phosphate head (hydrophilic region) and two glyceride tails (hydrophobic region). The major hydrophobic area of the two-layered structure, known as the lipid bilayer, is formed by the diglyceride tails, which are repelled from the cytoplasm and the extracellular matrix (ECM), while the phospholipid heads are in touch with either the cytoplasm or the ECM. Ion channels, surface receptors, enzymes, and hormones are some of the other biological components of a cell membrane that are crucial in controlling cellular activity and structural integrity.

A cell wall, which serves as an extra structural boundary outside the cell membrane and provides stiffness and resistance to mechanical stresses, is found in some cell types, such as bacteria and fungi. For instance, the peptidoglycans (10–80 nm) that make up the cell walls of bacteria are vital to their survival and are present in higher (90%) or lower (10%) concentrations in Gram-positive and Gram-negative strains, respectively. All bacterial and fungal cell walls generally contain proteins and polysaccharides, which vary significantly between taxonomic groupings and act as signaling signals to the cells, instructing them to modify their biophysical characteristics in response to external stimuli.

## 4 Mechanobiology behavior of cells within microfluidic devices

Microfluidic platforms are becoming increasingly important to understand the response of cells in various tissues under the influence of mechanical forces, also known as mechanotransduction [32]. However, mechanobiological effects can also be linked to intercellular tensions caused by active cell contraction, even when no external volume forces are present. This is the case with fluid shear stress, which is a common example of an externally imposed mechanical force. In this section, we have described the mechanotransduction concept in process simulation, where mechanical inputs are coupled with biological outputs. This can also alter the intrinsic mechanical properties of cells. The biological outcomes can also change in the microcellular environment, depending upon the type of mechanical inputs. This section presents an overview of the mechanical responses by different cell types and the microfluidic assays developed for probes associated with the biological responses. We have also explained some of the biological insights that were gained from these microfluidic assays.

### 4.1 Microfluidic devices for vasculature system: shear flow

Endothelial cells line the interior of blood vessels, making up the vasculature system. The external surface of blood cells includes erythrocytes, leukocytes, monocytes, and platelets and surrounds stromal cells, which comprise smooth muscle cells and pericytes. The blood arteries carry these cells around. The cells within the body are put through a variety of mechanical forces, including solid stresses and hemodynamic forces. The hemodynamic force, which interacts with the ECM and is characterized in terms of the shear stress produced by blood flow through the vessels, is the most important of these forces. Researchers recently developed a shearing-stretching apparatus to simulate a blood channel, which allowed them to analyze cell behavior under the impact of Stokes flow (low Reynolds number hydrodynamics) and explain how mechanical stimuli affected bovine aortic endothelial cells (BAECs). This gadget provided flexible mechano-environments by supplying shear flow and substrate stretching, separately or simultaneously [33]. Further, numerous microfluidic systems that accurately recreate important characteristics of the *in vivo* flow environment have been developed, all of which are based on a parallel flow chamber [34] and a cone plate viscometer [35]. Parallel plate flow chambers have experimentally demonstrated that fluid shear stress affects extracellular proliferation, migration, permeability, morphology, and gene expression of cells within the macroscale system [36]. The construction, mechanical control, and chemical analysis of microfluidic devices were significantly more effective and affordable when compared to the conventional *in vitro* microfluidic systems [33]. For instance, the development of realistic models based on microfluidic devices and advanced microfabrication technologies has improved our knowledge regarding biomolecules and cells in the vascular system, under diverse mechanical conditions [34, 35, 37].

Although the macroscale systems elucidate the response of endothelial cells under the influence of shear flow, these outcomes are unrealistic due to the large volumes of reagents and high cell numbers required. Thus, these systems have low experimental efficiency since only one shear stress level can be formed in each apparatus. These issues may be overcome by employing microfluidic platforms. Microfluidic devices have been designed so that multiple shear stress levels can be applied to the ECM used in the organ-on-chips to increase the experimental efficiency [38, 39]. For example, Song et al. discussed

multichannel shear flow-based microfluidic platform that allowed the simultaneous generation of different levels of pulsatile shear flows in each microfluidic channel. Pulsatile shear flows typically depict the arterial blood flow, which can be generated by an array of braille pins that help to drive the flow through the PDMS microchannels. The shear flow experiment's throughput was further boosted by a more advanced microfluidic device that made it possible to create ten different non-pulsatile shear stress levels (0.07–13 Pa) within a single chip. In other words, as the magnitude of shear stress is increased, the von Willebrand secretion by the ECM also increases. The magnitude of different cells under the influence of mechanical stimuli has been described in Table 2 [40].

In addition to these two systems, by narrowing the microchannel diameters, various microfluidic platforms have been developed to generate shear stress gradients within one microchannel [64, 65]. Within a single microchannel system, these platforms have been studied to better understand the effects of various shear stresses and their gradients on the ECM.

Along with shear flow, the ECM in the body system also encounters transendothelial flow, in which forces act on the mass transport across the extracellular monolayer. It is possible to trace the transendothelial flow close to a tumor or inflamed tissues [66]. Three-dimensional collagen hydrogels have been used in several microfluidic devices to study how transendothelial flow affects sprouting angiogenesis. Transendothelial flow is

**Table 2** The magnitude of different cells under the influence of mechanical stimuli

Stimulus	Cell type	Magnitude	Reference
Shear stress	Endothelial cells	0.07–13 Pa	[41]
	Platelets	0.05–5 Pa	[42]
	Erythrocytes	0.4–3.3 Pa	[43]
	Bone	0.007–0.24 Pa	[44]
	Lung	10 Pa	[45]
	Kidney	0.01 Pa	[46]
Interstitial flow	Endothelial cells	Interstitial flow: 1.7–11 $\mu\text{m/s}$	[47–49]
	Cancer cells	0.1–4.7 $\mu\text{m/s}$	[50]
Substrate strain	Stem cells	5% stretch, 1 Hz	[51–53]
	Cardiomyocytes	10% uniaxial strain	
	Kidney epithelium	~7%	
Substrate strain and lung shear stress	Lung	5–15% substrate strain at 0.2 Hz 0.01 Pa shear stress	[54]
	Gut	10% substrate strain at 0.15 Hz, 0.002 Pa shear stress	[55]
Confinement	Neurons	3 $\mu\text{m}$ high $\times$ 10 $\mu\text{m}$ wide	[56]
	Cancer cells	Collagen type I	[57, 58]
	Endothelial cells	100–200 $\mu\text{m}$ wide	[59]
Compression	Neurons	65 Pa (hippocampal)–540 Pa (DRG) maximum pressure before injury	[60]
Stiffness	Neurons	57–797 (Pa)—gradients ~0.5 Pa/ $\mu\text{m}$	[61]
Force measurement	Skeletal muscle cells, cardiomyocytes	0.2–0.45 mN/mm post stiffness Force generated: ~6–11 $\mu\text{N}$ (passive tension) 1–6 $\mu\text{N}$ (additional tension upon activation)	[62]
Flow generation	Cardiomyocytes	0.2–2 nL/min (theoretical 0.5 $\mu\text{L}/\text{min}$ )	[63]

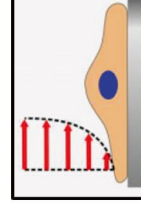
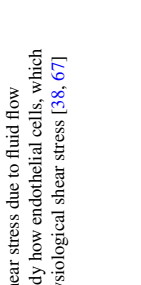
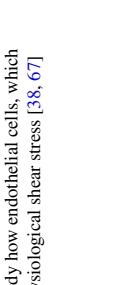


formed under the influence of hydrostatic pressure gradient across the collagen gel. For recapitulating the pulsatile flow in the vasculature system, in order to recreate the substrate strains that vascular cells in the body encounter, Zhou et al. reported a microfluidic device. This platform was used to investigate how mesenchymal stem cells responded to the changes in strain rate. The authors described cell alignment in their research work for strains > 10% [53]. Multiple investigations have been conducted to understand the effect of shear stress, cyclic strain, and soluble signals on the ECM. A novel microfluidic system was designed to operate under the influence of both, shear and stretch forces, on a co-cultured construct involving the ECM. Cells were grown in this system on an elastic membrane inside a PDMS microchannel. Vacuum pressure caused a 5% stretch in the membrane at a frequency of 1 Hz in flaking gas grooves, while the micropump applied shear stress of 2.6 Pa. The authors reported that the extracellular adhesion to the stem cell layer increased when both cell types were influenced by cyclic stretch and shear stress, respectively. This effect would not have been observed in the absence of substrate strain in the integrated microfluidic platform. Thus, this concept may stimulate the future development of novel microfluidic systems based on the application of multiple mechanical responses in co-culture systems. The effect of various mechanical stimuli within microfluidic devices and the resulting biological responses of cells and tissues have been listed in Table 3 [40].

#### 4.2 Case study: mechanobiology concept in organ-on-a-chip platform

The intervertebral disc (IVD) is a cartilaginous structure in the spinal cord, situated between two adjacent vertebrae. The annulus fibrosus (AF) surrounds the core nucleus pulposus (NP), which anatomically constitutes the IVDs. Hyaline cartilage endplates (CEPs) connect IVDs to the adjacent vertebrae [71–73]. The IVD is flexible enough to allow spinal motions and has the essential mechanical qualities to support the body's weight. An imbalance between anabolic and catabolic activities develops during IVD degeneration, which results in ECM deterioration and functional alterations. When these changes are accompanied by ongoing pain and inflammation, it is called degenerative disc disease (DDD) [74]. The IVDs are frequently subjected to a variety of mechanical loadings, such as compression, tension, shear, torsion, and their mixtures. In the mechanobiological reactions of the IVDs, the spinal loading and PG content are important factors [73]. This mechanical loading affects the IVD's physical environment by changing the ECM and cells' water content and chemical makeup [73, 75]. Depending on the size, frequency, and duration of the loading, mechanical stimuli cause cellular reactions in the IVDs, at a frequency between 0.2 and 1 Hz and magnitude between 0.2 and 0.6 MPa. The spinal stresses physiologically compress the IVDs [73].

OoCs are being developed to understand the functional anatomy, mechanobiology, and alterations that occur in IVDs, during progression of DDDs. To simulate human IVD pathophysiology, regulated physical stimulation must be included *in vitro*. OoCs offer several advantages over macroscale models, including the ability to precisely regulate fluid flow conditions and process parameters. The channel's small size ensures that the fluid flow is laminar (the Reynolds number ( $Re$ ) in microfluidic channels can be as low as 1), which enhances the ability to regulate the microscale phenomena and facilitates the prediction of experimental conditions [71]. If the explants' dimensions are suitable for a microscale system, improved control over fluid flow and, consequently, over the concentration of solutes and metabolites is also useful for sustaining *ex vivo* explants. In order to

**Table 3** Various mechanical stimuli within the microfluidic device and their effect on cell responses

Types of mechanical stimuli	Description	Schematic diagram of resulting cell response
Shear Stress	Cells developed inside the microfluidic devices under the influence of shear stress due to fluid flow behavior through narrow confinement. These platforms are used to study how endothelial cells, which align themselves in the direction of fluid flow under the scheme of physiological shear stress [38, 67]	
Interstitial flow	The influence of interstitial flow behavior on cell migration and cell alignment are studied here by considering the fluid pressure gradient within the hydrogel. For instance, this platform allowed the parameters governing upstream and downstream movement in response to flow behavior to be clarified when interstitial flow (blue arrow) was applied to cancer cells seeded within a collagen hydrogel [68]	
Stiffness gradient	Gradients in stiffness of a substrate within a microfluidic device are used to study the effect of stiffness gradient on axon outgrowth, axons grow more preferentially in the direction of decreasing stiffness [60]	
Force measurement	To quantify the force produced by mechanically active tissues and cells, devices have been developed. Within the two micro-cantilevers in this example, cardiac microtissue was grown. It was possible to measure the force produced by muscle tissue by observing how the cantilevers moved as the muscle tissue contracted [69]	
Stretching	Devices have been developed here to investigate the impact of mechanical stretch on the cells cultured on the deformable substrate by integrating flexible substrates into the microfluidic platforms [70]	

accommodate complete mouse lumbar IVDs (8–10 weeks old), a microfluidic disc-on-a-chip with continuous media flow was created [76].

Numerous studies have demonstrated that physiological compression and stretching encourage the production of IVD-like ECM. The effects of shear stress in IVD, however, are often little studied. Chou et al. (2016) offered preliminary evaluation of the direct impact of shear stresses on human AF cells, in a microfluidic environment. In the beginning, a double-sided tape was used to attach a polymethylmethacrylate (PMMA) pre-culture chamber to a substrate that was coated with fibronectin. Following the adhesion of AF cells to the substrate, it was removed from the growth chamber and integrated into the five-layer device. Fluid flow was facilitated via an inlet and an outlet, and the culture substrate was joined to the rest of the device by a vacuum inlet that applied negative pressure. In this study, after overnight incubation at 37 °C, the authors used hAF cells on the Fn-coated bio-microfluidic device, which had a similar morphology to cells cultured in a dish. Once the cells were ready, the entire bio-microfluidic device was assembled by assembling the laser-cut dishes with the microfluidic chips using vacuum force. It was observed that the hAF cells reacted to the shear stress that was applied. The research aided in the creation of a new therapeutic approach for IVD degeneration as well as the understanding and clarification of the effects of shear stress on IVD degeneration [77].

## 5 Cell stimulation and microfluidics

Microfluidic systems are also being employed to conduct fundamental investigations in cell biology. By observing how cells react to controlled perturbations in the extracellular micro-environment, we can get biological insights into the molecular mechanisms that regulate cell phenotypic behavior. As a result, a vast array of microsystems have been developed to specifically support the fundamental studies into biochemical processes, cell fate determination, and tissue morphogenesis. In this section, we will discuss several more applications of cell-based assays that can be performed with microfluidic devices and understand a few unit operations (i.e., cell lysis, cell separation, and analysis of cells) which are very useful concepts to fabricate, integrate, and pack the microfluidic device. Readers are also referred to more detailed reviews regarding cell stimulation and microfluidics [78–85].

### 5.1 Stimulation of adherent cells

Controlled perturbations in the cellular microenvironment, as a function of time and space, for adherent cells within a microfluidic device can be achieved by controlling the flow rate of the medium being circulated in the device. In the case of laminar flow, diffusive mixing occurs within the microfluidic channels, which can be used to create complex concentration gradients that are not possible to achieve within macroscale devices [86]. These concentration gradients allow several conditions that are experienced *in vivo* to be probed simultaneously. For example, in split and recombine micro-mixers, a complex concentration gradient is formed due to the lamination and splitting of the fluid streams, which promotes cellular chemotaxis [32]. Some biases have been observed in the case of cell migrations under the influence of shear forces having high volumetric flow rates. Linear gradients of concentration distribution have been observed under static conditions (convection-free) microfluidic systems. These are also observed

without perturbing the existing distribution of secreted molecules. For cell culture applications, gradient generation permits several growth conditions which need to be analyzed in a combined manner [32].

In a system with rapid flow and large molecules having smaller diffusion coefficients, the diffusion process is slow under the influence of any appreciable mixing between the fluid streams. Slow diffusive mixing offers the chance to change the liquid phase environment at distances comparable to cell size, even though slow diffusion can cause complications in processes where mixing is crucial. As for example, pulsatile blood flow and pulsating pressure cause blood vessels to be regularly exposed to a variety of hemodynamic forces, including flow-dependent shear stress (FSS). The cellular structures like the cell membranes respond to this mechanical stimulus by bringing about a change in their shapes. Taking this into account, it was observed that human dental pulp stem cells (hDPSCs) exposed to FSS (dynamic flow conditions) reorganized their morphology. The cells changed their fibroblast-like shape (in static condition, where the media flow is not accounted for) to obtain a more elongated morphology (in dynamic condition, where the media flow is considered), as depicted in Fig. 2 [87]. A similar approach was used to generate a temperature gradient instead of a complex concentration gradient, where the effects of temperature perturbations over embryonic development were studied [88]. In the context of stimulation associated with adherent cells, controlled perturbations are important parameters that can be regulated by the flow rate of the medium. So, perfusion-based microfluidic devices (fluid convection is accounted for) are better as compared to static devices (i.e., commercially available trans wells or cell culture inserts or in-house fabricated PDMS-based devices, etc.) because we can precisely control the microenvironment surrounding the cells that allow for more uniform cell behavior and the ability to study cells under more physiologically relevant conditions.

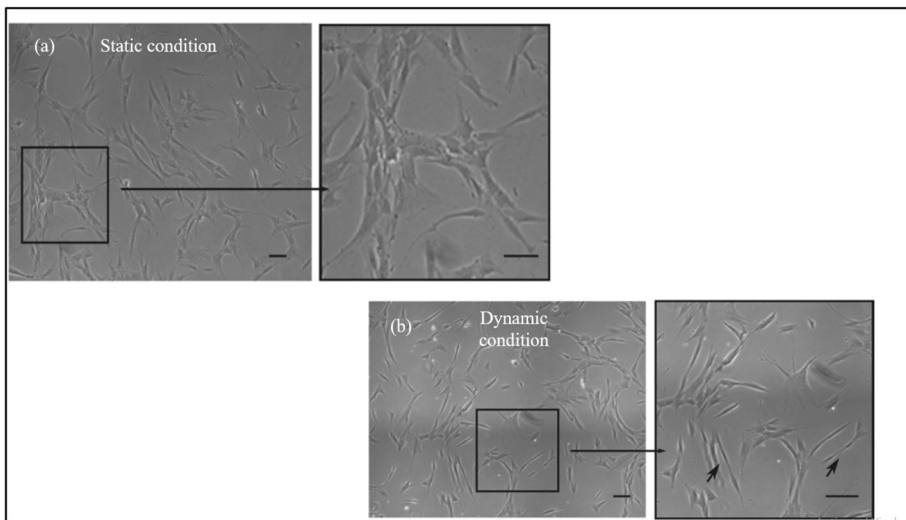


**Fig. 2** Morphology characterization of hDPSCs after culturing them in static and dynamic conditions. Squares show magnification of a small part of the image, while arrows demonstrate morphology characteristics. Adapted from [87]

## 5.2 Cell stimulation in suspension

In a suspension system, cells are transported under the influence of an adverse pressure gradient of the flow rate of the cell culture medium within the microfluidic devices. However, filters and traps can physically retain the cells within the devices. In the case of the hydrodynamic traps, cells are retained in a fixed position by combining the effect of concentration gradients and the flow of cells. A microfluidic system was used to track ATP-dependent calcium uptake in HL-60 cells during cell stimulation in suspension [89]. Cells were captured using hydrodynamic traps on both sides of the microfluidic channel, facilitating well-defined cell-to-cell interaction. The cells spent a specific amount of time in each microfluidic compartment if they were permitted to migrate through the microfluidic channel along with the bulk liquid, such as nutrient media or buffer solutions. By establishing a microcirculation within each section of the microfluidic compartment, flow segmentation was used to improve the mixing process [90].

## 5.3 Cell sorting within the microfluidic device

In the case of fluid transport, which involves selective trapping and diversion of suspended cells, a cell sorting device was integrated into the microfluidic system and was used as an essential tool for cell stimulation. It was crucial to be able to separate a concentrated and homogeneous cell suspension from a heterogeneous cell mixture in order to get precise data on the underlying biochemistry of particular cell types in the combination. Microfluidic technology was used to separate a few cells or even a single cell from a large population of cells based on specific properties, like electrical properties and fluorescent markers [28]. In the case of cell sorting devices, electrodes were placed within the microsystems and produced a dielectric force to move, separate, and position the individual cells. The induced dipoles in the cells produced dielectric force (DEP), which was then exposed to a non-uniform electrical field. The DEP was dependent on the inherent characteristics of cells, such as the capacitance and conductance of the membrane. Both characteristics were affected by the type of cell and even by cell activation. For instance, under the influence of the DEP force, MDA231 cancer cells were separated from dilute blood samples by selective capture at the microelectrodes, which were placed over the outer surface of the microfluidic devices. Tagging cells using marker particles with different dielectric properties was also performed under the influence of DEP force to separate rare cells, at the rate of 10,000 cells/s, with an enrichment factor of 200 [90]. Based on the electrode design, DEP force was also employed to capture selective cells for further analysis. The importance of cell populations before biochemical analysis was explored under the influence of the DEP force and was used to separate two different cells, i.e., U937 cells and peripheral blood mononuclear cells, into two homogeneous populations. Transient adhesion between the cells and appropriate surfaces retarded their movement through the microfluidic channels. This occurred due to the chromatographic separation between two cell types based on the difference in their retardation.

Many microfluidic cell sorting devices can be integrated with microelectrodes, microvalves, and even micropumps. Most microfluidic systems rely on bulk optical elements like lenses and microscopes, for optical control and detection. Miniaturization of the optical components is not easy to integrate within the microfluidic platforms.



Recently, integrated polymer waveguides and lenses were described for use with microchip-based flow cytometers [91].

## 5.4 Cell lysis using microfluidic devices

On a laboratory scale, cell lysis is often conducted either chemically, by utilizing detergents, or mechanically, by rupturing membranes. Either of these approaches can be integrated into microfluidic devices. Microdevices have successfully used both chemical lysis with Triton X-100 and denaturation with SDS (sodium dodecyl sulfate). The fundamental benefit of using cell buffers to achieve chemical lysis in microdevices is that they may be tailored for traditional biological experiments. An alternate technique is mechanical cell lysis, which involves detergent-mediated cell lysis followed by downstream analysis. Microscale shear lysis technique is like the traditional microscopic method, in which force was applied over HL-60 cells through nanoscale barbs [92]. Cell lysis can also be mediated through application of electric field inside the microchannels, as depicted in Fig. 3 [93–95]. In this case, as shown in Fig. 3, the device design has two perpendicular cross channels with varying widths along the horizontal direction (labeled as sections 1, 2, and 3). Sections 2 and 3, particularly, are used for electrical cell lysis and electrophoretic separation of cell contents, respectively. Electrical lysis can be rapid, with a low disruption time scale (33 ms), and is about eight times faster as compared to chemical lysis phenomena. Microfabricated electroporation may additionally destabilize the cell membrane reversibly, during gene transfection processes, by carefully regulating the electrical field's strength [96].

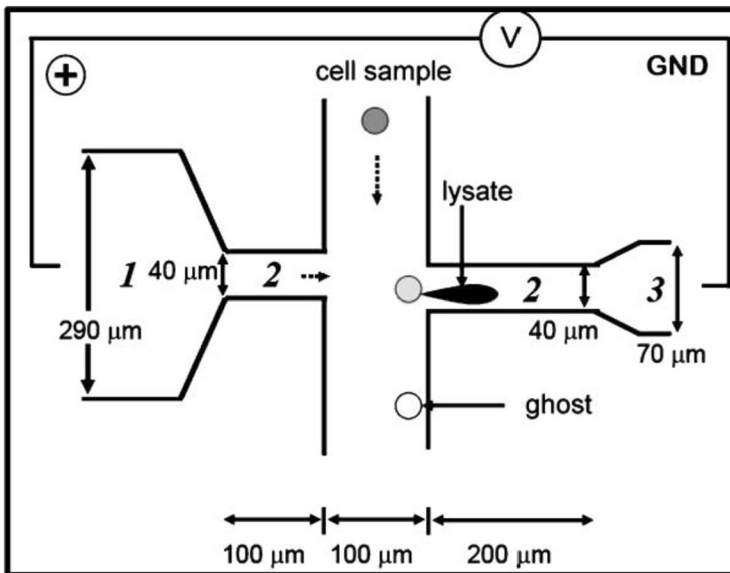


**Fig. 3** Schematic diagram of electrical lysis of cells with pressure-driven flows for cell cytometry (adapted from [97] with permission from Elsevier)

## 6 Case study: manipulation of cancer cells in microfluidic systems

Cell biology and microfluidics have been combined to manipulate and analyze rare cells, such as stem cells, fetal cells, and cancer cells. Such a lowering of system dimensions, combined with precision manipulation technologies, has enabled accurate and affordable investigations about cellular bioprocesses using low sample sizes and parallelization. It is intriguing to consider the possible contributions that these technologies could make to advance our understanding of cancer biology, from label-free on-chip flow cytometry and micro-sorting procedures to molecular processes of drug resistance and drug development. Microfluidics is quickly emerging as a crucial tool for many researchers engaged in cancer research.

### 6.1 Deformability and migration studies

In response to changes in external stimuli, cancerous cells are better able to modify their migratory processes as compared to non-cancerous cells [24]. This prompted researchers to develop methods for immobilizing cancer cells by blocking signal transduction pathways to study migratory mechanisms. Different cancer cell lines exhibit variations in migration speed and mode, and extracellular matrix-filled PDMS microchannels with pre-determined cell migration pathways for visual measurement have been used to identify these variations. Mesenchymal, amoeboid, and collective cell migration are the three types of cancer cell migration modes that have been reported in the literature. These can be distinguished by their morphology and movement traits in response to soluble chemokines, ECM, and surface stimuli [98]. The high deformability of a cancer cell's cytoskeleton is one of the primary reasons for its capacity to migrate in small 3D spaces [99]. Investigations of the deformation of benign and malignant breast cancer cells using microchannel constrictions were performed in 2009 [100]. It was shown that metastatic cells had a faster entry time into the channel, which might be used as a label-free biomarker to discriminate between cancer-free and cancer-affected cells. Targeting and enriching MCF-7 cells spiked in peripheral blood, using inertial focusing and deformability-induced migration, was demonstrated using a passive high-throughput cell classification method that was only based on size and deformation properties [101]. Cells immobilized using adhesion molecules like cadherins on the coated surfaces of channel walls or micropillars within the channels of microfluidic devices have also been used to study the effects of hydrodynamic loading, chemotaxis, and electrotaxis on mechanical interactions between the substrate and the migrating cell. To properly recreate the migration properties, these cells were also evaluated with fluid hydrodynamic flow applied electric fields, as well as other chemoattractants, in gradient or diffusion-based flows [102–104].

### 6.2 Microfluidic separation and sorting

It was shown that the right channel lengths could only achieve the equilibrium of cancer cells at up to 10% hematocrit volume, which was suggested to help with the development of microfluidic separators [105]. This made it possible to create a separation method without using cell surface indicators like epithelial cell adhesion molecules (EpCAM). Based on their respective cell cycle phases, human liver cancer cells (HepG2) and fibroblasts (NIH/3T3) were separated, demonstrating HDF's promise as a potent damage-free separation method in cellular genetics [106]. Additionally, with 95.5% and 85.2% efficiency, respectively, researchers used hydro-phoretic sorting to separate an asynchronous

population of human leukemic monocyte lymphomas into the  $G_0/G_1$  and  $G_2/M$  cell cycle stages [107]. Mammalian cell acoustophoretic cell synchronization (ACS) was demonstrated in the year 2010 [108]. The size-dependent phases of an asynchronous sample of MDA-MB-231 human breast cancer cells were separated, with bigger cells in  $G_2/M$  and S phases flowing more quickly to the central stream (output A) than the smaller cells in the  $G_1$  phase (output B). Approximately 84% of  $G_1$  phase synchronization was attained using this method.

Using a disposable microfluidic device and currents up to 1 Amp, iterative microsystem optimization was used to separate CD133+ or MCF-7 carcinoma cells from human blood, producing results with high purity and >96% separation efficiency. The processing of clinical samples for the extraction, separation, and analysis of circulating tumor cells (CTCs), hematopoietic stem cells (HSC), or endothelial progenitor cells (EPC) has gained momentum using magnetophoretic microfluidic devices [109, 110]. While in situ biofunctionalization with a glycoprotein and washing of beads occurred close to the pillars, superparamagnetic (SPM) beads were effectively confined between magnetized pillar arrays. When used in the ratio of 1:10 of cancer to red blood cells (RBCs), A549 cells caught in the pillar arrays and then released at the outlet were enriched by a factor of 133 [111]. Saliba and colleagues [112] modified a reported method [111] in which magnetic traps created by microcontact printing were magnetized and biofunctionalized with SPM beads, self-assembled into microarray columns. Jurkat (CD19 neg) and Raji (CD 19 pos) cells were successfully collected with an efficiency >94%, using flow-activated cells and interactions with the SPM beads, followed by an effective in situ on-cell culture right after sorting. These techniques, which utilized biofunctionalized SPM beads as a fixed platform to gather unlabeled cells, constituted a significant departure from the often used freely suspended multi-targeted immunomagnetic activation method [113].

Recently, label-free cells in a flow-focused paramagnetic ionic solution were separated using a tuneable magnetophoretic separation device [114]. Red blood cells (RBCs) and human lymphoma monocytes (U937) were separated by repulsive forces. Despite their poor throughput, the diamagnetic particles were driven away from the magnet at varying magnetophoretic mobility rates that depended upon the cell size and magnetic susceptibility.

### 6.3 Current challenges in sorting and detection

High-throughput microfluidic flow cytometry tools compete with the more intricate, pricey, and larger fluorescence-activated cell sorting (FACS) flow cytometers by focusing, counting, detecting, or sorting cells on a single chip. Since the introduction of  $\mu$  FACS in 1999 [115], numerous activated cell sorting microdevices reliant on dielectrophoresis (DEP), Raman spectroscopy (RACS), hydrodynamics, and magnetic susceptibilities (MACS), as well as synthetic labels for altering the complicated permittivity of multitarget cells (MT-DACS), have been explained. Some of these devices can separate cancerous and non-cancerous cells with efficiencies of >85% or throughputs of up to 10,000 cells per second [93, 116–121]. With the exception of FACS and MACS, these novel microflow cytometers, which have been evaluated using malignant cells, do not require pre-labeling but sort cells based solely on their intrinsic characteristics like size, dielectric constant, deformability, and refractive index. Importantly, if these novel microsystems are to be utilized as substitutes to sheath-based, high-speed quantification and sorting by FACS, problems with regard to throughput, improved sensitivity, and incorporation of actuating mechanisms should be overcome and validated before their adoption in clinical settings may be endorsed.

## 7 Conclusions and future prospects

Microfluidic systems have been developed to facilitate both applied and basic research with cells and tissues. Integration and automation are important to develop microfluidic devices for cell biology-related applications. In terms of reproducibility, managing smaller sample sizes, and high-throughput experimentation, these can offer improved precision. Integrated microfluidic systems should be created in the future to provide exact biochemical and mechanistic data from cells and tissues, as opposed to only basic phenotypic alterations. Automation of such integrated devices may avoid processing of the samples before introduction into the microfluidic device. For example, a fully integrated liver toxicology chip might support a 3D micro-culture of hepatocytes consisting of distinct phenotypes and fluidic approaches. This would allow a continuous flow of culture media and exposure of cells to biological or small chemicals. Online separators would segregate specific cell populations within the cell lysis chambers. In addition to the online cell separators, multiplexed online sandwich immunoassays can be integrated with optics and level-free detection to detect cell separation. This system will require lesser material, as compared to the laboratory-scale methods, and can offer significant advantages to primary cells and patient tissues.

Cell stimulation studies, under static and dynamic conditions, are important as various biological processes, such as cell differentiation, proliferation, and migration, depend upon different mechanical forces acting on the cells. Similarly, cell sorting and lysis enable researchers to manipulate the cells on chips. Cells can be precisely manipulated within microfluidic devices prepared using microfabrication technology, which may permit characterization of individual cells, their lysis, and detection. Microfluidic devices also enable handling of very small sample volumes, which simplifies single cell analysis. This capability is valuable in deciphering cellular heterogeneity and understanding individual cell response within a heterogeneous population. With regard to the biomedical applications, microfluidic cell stimulations have found applications in diverse biomedical areas, including drug discovery, toxicology studies, cancer research, tissue engineering, and regenerative medicine. While microfluidic cell stimulations offer numerous advantages, there are also some drawbacks and challenges that need to be addressed for their continued development and broader adoption. In case of cell computability, certain cell types may not readily adapt to microfluidic environments and the behavior of cells within the devices might not fully represent their natural *in vivo* responses. To fully exploit the benefits of microfluidic cell stimulations, integration with other analytical and imaging technologies is essential. However, development of compatible systems and data analysis can be complex.

Significant challenges have also been encountered in the case of routine cell culture applications using microfluidic devices, and the future chips should be comparable to the laboratory-scale technologies used to analyze complex cellular phenomena. Highly integrated microfluidic devices will find significant applications in basic and applied research, with the point-of-care portable devices also finding applications in clinical settings. A concentrated effort combining multiple manipulation methods is required to begin handling therapeutically relevant material. It could be claimed that Giddings laid down this foundation, but technological developments have had a significant impact on the design and optimization of microfluidic devices for diverse applications. If on-chip sample-making devices have to be included in fully automated laboratory on-chip (LOC) systems, for instance, handling blood samples (40% v/v hematocrit) makes it impossible for electrokinetic technologies with sample channel geometries to handle high, medium

conductivities. Through flow splitting and recombining with low ionic solutions, the integration of hydrodynamic filtration technologies may enhance downstream electrokinetic processing activities.

The major understanding of the molecular mechanisms underlying the cellular ability to respond to stimuli is heavily dependent on conventional macro-assays, even though microfluidic systems have been developed for examining the effects of mechanical forces on the cells. Microfluidic platforms, on the other hand, are a feasible way to capture intricate aspects of *in vivo* physiology, such as the co-culture of bacteria in the gut epithelium [70], neutrophil diapedesis through the lung epithelium [53], and apical-basal polarity in IMCDs [122]. Future developments in the microfluidic technology by integration of quantitative biochemical techniques will enable an in-depth study of cellular behavior and tissue properties, like *in vivo*-like permeability in the gut epithelial cells, because such cellular behaviors can be easily studied using microfluidic systems as these systems allow a precise control over the applied stimulus.

Mechanobiology studies using microfluidic device have significantly advanced our understanding of how mechanical forces influence cellular behavior and functioning. These devices provide a precise platform to investigate the mechanical cues on cells, tissues, and even organisms. Some of the major conclusions drawn from mechanobiology studies using microfluidic devices include following:

1. **Mechanotransduction pathways:** microfluidic devices have helped to identify and elucidate key mechanotransduction pathways that convert mechanical signals into biochemical responses within cells. This knowledge has shed light on various cellular processes, including cell adhesion, migration, differentiation, and gene expression.
2. **Cell substrate interactions:** microfluidic devices allow study of cellular interaction with specific substrates, such as ECMs and other engineered materials. These studies have provided insights into how cells sense and respond to the mechanical properties of their microenvironment.
3. **Tissue engineering applications:** by applying the mechanical forces in a controlled manner, microfluidic devices have facilitated tissue engineering studies. These include studies related to tissue growth, organization, and maturation, leading to the development of function tissue constructs for regenerative medicine. Additionally, mechanobiology studies using microfluidic devices have provided valuable insights into the mechanical basis of certain diseases. Understanding how mechanical forces contribute to disease progression can lead to new therapeutic approaches and interventions.

Despite the significant progress made in mechanobiology study using microfluidic devices, there are several future drawbacks and challenges that need to be considered for further advancements, such as the following:

1. **Integration of multiple mechanical cues:** *in vivo* cells experience a combination of mechanical cues, such as shear stress, compression, and stretch. Incorporating multiple mechanical stimuli into a single microfluidic device while maintaining cell viability and experimental control is a complex task.
2. **Multi-cellular systems:** while microfluidic devices have been successful in studying single cell responses, understanding the behavior of multi-cellular systems under mechanical forces presents additional challenges, including cell–cell interactions and tissue level responses.

In vitro models of mechanotransduction in living systems can also be improved by combining several existing technologies. For instance, utilizing embryoid bodies implanted in a 3D hydrogel, techniques creating tissue compression can be paired with matrix stretch and chemical gradients to imitate the processes taking place during development. Systems that allow for simultaneous shear flow and interstitial flow, possibly with various cell types, can also be developed for investigating the combined impact of surroundings on tumor cells, in case of a vascularized tumor. Such compound systems retain their tight control and real-time viewing capabilities, while offering some of the in vivo realism to the in vitro models. However, this may become a reality only if they can be simultaneously replicated in various laboratories investigating mechanobiology [40].

**Acknowledgements** Joydeb Mukherjee is thankful to Zydus Life Science Limited for providing the opportunity to work on this topic. Deepa Chaturvedi would like to thank the Department of Science and Technology (DST-Purse/1933).

**Author contributions** 1. Joydeb Mukherjee: Writing, editing the original draft. 2. Deepa Chaturvedi: Writing the original draft. 3. Shlok Mishra: Writing the original draft. 4. Ratnesh Jain: Writing, editing the original draft. 5. Prajakta Dandekar: Writing, editing the original draft.

## Declarations

**Competing interests** The authors declare no competing interests.

## References

- Gravesen, P., Branebjerg, J., Jensen, O.S.: Microfluidics—a review. *J. Micromech. Microeng.* **3**, 168–182 (1993). <https://doi.org/10.1088/0960-1317/3/4/002>
- Whitesides, G.M., Stroock, A.D.: Flexible methods for microfluidics. *Phys. Today* **54**, 42–48 (2001). <https://doi.org/10.1063/1.1387591>
- Becker, H., Gärtner, C.: Polymer microfabrication methods for microfluidic analytical applications. *Electrophoresis* **21**, 12–26 (2000). [https://doi.org/10.1002/\(SICI\)1522-2683\(2000101\)21:1%3c12::AID-ELPS12%3e3.0.CO;2-7](https://doi.org/10.1002/(SICI)1522-2683(2000101)21:1%3c12::AID-ELPS12%3e3.0.CO;2-7)
- Jakeway, S.C., de Mello, A.J., Russell, E.L.: Miniaturized total analysis systems for biological analysis. *Fresenius J. Anal. Chem.* **366**, 525–539 (2000). <https://doi.org/10.1007/s002160051548>
- Brody, J.P., Yager, P., Goldstein, R.E., Austin, R.H.: Biotechnology at low Reynolds numbers. *Biophys. J.* **71**, 3430–3441 (1996). [https://doi.org/10.1016/S0006-3495\(96\)79538-3](https://doi.org/10.1016/S0006-3495(96)79538-3)
- Squires, T.M., Quake, S.R.: Microfluidics: fluid physics at the nanoliter scale. *Rev. Mod. Phys.* **77**, 977–1026 (2005). <https://doi.org/10.1103/RevModPhys.77.977>
- Mala, G.M., Li, D.: Flow characteristics of water in microtubes. *Int. J. Heat Fluid Flow* **20**, 142–148 (1999). [https://doi.org/10.1016/S0142-727X\(98\)10043-7](https://doi.org/10.1016/S0142-727X(98)10043-7)
- Weilin, Q., Mala, G.M., Dongqing, L.: Pressure-driven water flows in trapezoidal silicon microchannels. *Int. J. Heat Mass Transf.* **43**, 353–364 (2000). [https://doi.org/10.1016/S0017-9310\(99\)00148-9](https://doi.org/10.1016/S0017-9310(99)00148-9)
- Ajdari, A.: Generation of transverse fluid currents and forces by an electric field: electro-osmosis on charge-modulated and undulated surfaces. *Phys. Rev. E* **53**, 4996–5005 (1996). <https://doi.org/10.1103/PhysRevE.53.4996>
- Dertinger, S.K.W., Chiu, D.T., Jeon, N.L., Whitesides, G.M.: Generation of gradients having complex shapes using microfluidic networks. *Anal. Chem.* **73**, 1240–1246 (2001). <https://doi.org/10.1021/ac001132d>
- Jeon, N.L., Dertinger, S.K.W., Chiu, D.T., Choi, I.S., Stroock, A.D., Whitesides, G.M.: Generation of solution and surface gradients using microfluidic systems. *Langmuir* **16**, 8311–8316 (2000). <https://doi.org/10.1021/la000600b>
- Jacobson, S.C., McKnight, T.E., Ramsey, J.M.: Microfluidic devices for electrokinetically driven parallel and serial mixing. *Anal. Chem.* **71**, 4455–4459 (1999). <https://doi.org/10.1021/ac990576a>
- Liu, R.H., Stremler, M.A., Sharp, K.V., Olsen, M.G., Santiago, J.G., Adrian, R.J., Aref, H., Beebe, D.J.: Passive mixing in a three-dimensional serpentine microchannel. *J. Microelectromech. Syst.* **9**, 190–197 (2000). <https://doi.org/10.1109/84.846699>

14. Byron Bird, M.R., Stewart, W.E., Lightfoot, E.N.: Transport phenomena. John Wiley & Sons (2006)
15. Fähreus, R., Lindqvist, T.: The viscosity of the blood in narrow capillary tubes. *Am. J. Physiol.* **96**, 562–568 (1931). <https://doi.org/10.1152/ajplegacy.1931.96.3.562>
16. Zharov, V.P., Galanzha, E.I., Menyayev, Y., Tuchin, V.V.: In vivo high-speed imaging of individual cells in fast blood flow. *J. Biomed. Opt.* **11**, 054034 (2006). <https://doi.org/10.1117/1.2355666>
17. Pipe, C.J., McKinley, G.H.: Microfluidic rheometry. *Mech. Res. Commun.* **36**, 110–120 (2009). <https://doi.org/10.1016/j.mechrescom.2008.08.009>
18. Stroock, A.D., Whitesides, G.M.: Controlling flows in microchannels with patterned surface charge and topography. *Acc. Chem. Res.* **36**, 597–604 (2003). <https://doi.org/10.1021/ar0202870>
19. Trietsch, S.J., Hankemeier, T., van der Linden, H.J.: Lab-on-a-chip technologies for massive parallel data generation in the life sciences: a review. *Chemom. Intell. Lab. Syst.* **108**, 64–75 (2011). <https://doi.org/10.1016/j.chemolab.2011.03.005>
20. Frank, M.: White: Fluid mechanics. McGraw-Hill International Edition, New York (1994)
21. Cornish, R.J.: Flow in a pipe of rectangular cross-section. *Proc. R. Soc. Lond. Ser. A Contain. Pap. Math. Phys. Character* **120**, 691–700 (1928). <https://doi.org/10.1098/rspa.1928.0175>
22. Beebe, D.J., Mensing, G.A., Walker, G.M.: Physics and applications of microfluidics in biology. *Annu. Rev. Biomed. Eng.* **4**, 261–286 (2002). <https://doi.org/10.1146/annurev.bioeng.4.112601.125916>
23. Fuerstman, M.J., Lai, A., Thurlow, M.E., Shevkopyas, S.S., Stone, H.A., Whitesides, G.M.: The pressure drop along rectangular microchannels containing bubbles. *Lab Chip* **7**, 1479 (2007). <https://doi.org/10.1039/b706549c>
24. Li, X. (James), Zhou, Y.: Microfluidic devices for biomedical applications. Woodhead Publishing Limited, Cambridge, England (2013)
25. Folch, A., Toner, M.: Microengineering of cellular interactions. *Annu. Rev. Biomed. Eng.* **2**, 227–256 (2000). <https://doi.org/10.1146/annurev.bioeng.2.1.227>
26. Veenstra, T.T., Lammerink, T.S.J., Elwenspoek, M.C., van den Berg, A.: Characterization method for a new diffusion mixer applicable in micro flow injection analysis systems. *J. Micromech. Microeng.* **9**, 199–202 (1999). <https://doi.org/10.1088/0960-1317/9/2/323>
27. Gregory, T.A.: Kovacs: Micromachined transducers sourcebook. WCB/McGraw-Hill, Boston (1998)
28. El-Ali, J., Sorger, P.K., Jensen, K.F.: Cells on chips. *Nature* **442**, 403–411 (2006). <https://doi.org/10.1038/nature05063>
29. Kutluk, H., Bastounis, E.E., Constantinou, I.: Integration of extracellular matrices into organ-on-chip systems. *Adv. Healthc. Mater.* (2023). <https://doi.org/10.1002/adhm.202203256>
30. Prins, M.W.J., Welters, W.J.J., Weekamp, J.W.: Fluid control in multichannel structures by electrocapillary pressure. *Science* **1979**(291), 277–280 (2001). <https://doi.org/10.1126/science.291.5502.277>
31. Alberts, B., Johnson, A., Lewis, J., Raff, M., Roberts, K., Walter, P.: Molecular biology of the cell. Garland Science, New York (2002)
32. Helmke, B.P., Minerick, A.R.: Designing a nano-interface in a microfluidic chip to probe living cells: challenges and perspectives. *Proc. Natl. Acad. Sci. U.S.A.* **103**, 6419–6424 (2006). <https://doi.org/10.1073/pnas.0507304103>
33. Young, E.W.K., Simmons, C.A.: Macro- and microscale fluid flow systems for endothelial cell biology. *Lab Chip* **10**, 143–160 (2010). <https://doi.org/10.1039/B913390A>
34. Lee, J., Huh, H.K., Park, S.H., Lee, S.J., Doh, J.: Endothelial cell monolayer-based microfluidic systems mimicking complex in vivo microenvironments for the study of leukocyte dynamics in inflamed blood vessels. Presented at the (2018)
35. Skorupska, S., Jastrzebska, E., Chudy, M., Dybko, A., Brzozka, Z.: Microfluidic systems. In: *Cardiac Cell Culture Technologies*. pp. 3–21. Springer International Publishing, Cham (2018)
36. Li, Y.-S.J., Haga, J.H., Chien, S.: Molecular basis of the effects of shear stress on vascular endothelial cells. *J. Biomech.* **38**, 1949–1971 (2005). <https://doi.org/10.1016/j.jbiomech.2004.09.030>
37. Castiaux, A.D., Spence, D.M., Martin, R.S.: Review of 3D cell culture with analysis in microfluidic systems. *Anal. Methods* **11**, 4220–4232 (2019). <https://doi.org/10.1039/C9AY01328H>
38. Song, J.W., Gu, W., Futai, N., Warner, K.A., Nor, J.E., Takayama, S.: Computer-controlled microcirculatory support system for endothelial cell culture and shearing. *Anal. Chem.* **77**, 3993–3999 (2005). <https://doi.org/10.1021/ac050131o>
39. Chau, L., Doran, M., Cooper-White, J.: A novel multishear microdevice for studying cell mechanics. *Lab Chip* **9**, 1897 (2009). <https://doi.org/10.1039/b823180j>
40. Polacheck, W.J., Li, R., Uzel, S.G.M., Kamm, R.D.: Microfluidic platforms for mechanobiology. *Lab Chip* **13**, 2252 (2013). <https://doi.org/10.1039/c3lc41393d>
41. Lam, R.H.W., Sun, Y., Chen, W., Fu, J.: Elastomeric microposts integrated into microfluidics for flow-mediated endothelial mechanotransduction analysis. *Lab Chip* **12**, 1865 (2012). <https://doi.org/10.1039/c2lc21146g>

42. Gutierrez, E., Petrich, B.G., Shattil, S.J., Ginsberg, M.H., Groisman, A., Kasirer-Friede, A.: Microfluidic devices for studies of shear-dependent platelet adhesion. *Lab Chip* **8**, 1486 (2008). <https://doi.org/10.1039/b804795b>
43. Moehlenbrock, M.J., Price, A.K., Martin, R.S.: Use of microchip-based hydrodynamic focusing to measure the deformation-induced release of ATP from erythrocytes. *Analyst* **131**, 930 (2006). <https://doi.org/10.1039/b605136g>
44. Jang, K., Sato, K., Igawa, K., Chung, U., Kitamori, T.: Development of an osteoblast-based 3D continuous-perfusion microfluidic system for drug screening. *Anal. Bioanal. Chem.* **390**, 825–832 (2008). <https://doi.org/10.1007/s00216-007-1752-7>
45. Huh, D., Fujioka, H., Tung, Y.-C., Futai, N., Paine, R., Grotberg, J.B., Takayama, S.: Acoustically detectable cellular-level lung injury induced by fluid mechanical stresses in microfluidic airway systems. *Proc. Natl. Acad. Sci. U.S.A.* **104**, 18886–18891 (2007). <https://doi.org/10.1073/pnas.0610868104>
46. Baudoin, R., Griscom, L., Monge, M., Legallais, C., Leclerc, E.: Development of a renal microchip for in vitro distal tubule models. *Biotechnol. Prog.* **23**, 1245 (2007). <https://doi.org/10.1021/bp0603513>
47. Song, J.W., Munn, L.L.: Fluid forces control endothelial sprouting. *Proc. Natl. Acad. Sci. U.S.A.* **108**, 15342–15347 (2011). <https://doi.org/10.1073/pnas.1105316108>
48. Hsu, Y.-H., Moya, M.L., Hughes, C.C.W., George, S.C., Lee, A.P.: A microfluidic platform for generating large-scale nearly identical human microphysiological vascularized tissue arrays. *Lab Chip* **13**, 2990 (2013). <https://doi.org/10.1039/c3lc50424g>
49. Shields, J.D., Fleury, M.E., Yong, C., Tomei, A.A., Randolph, G.J., Swartz, M.A.: Autologous chemotaxis as a mechanism of tumor cell homing to lymphatics via interstitial flow and autocrine CCR7 signaling. *Cancer Cell* **11**, 526–538 (2007). <https://doi.org/10.1016/j.ccr.2007.04.020>
50. Svennersten, K., Berggren, M., Richter-Dahlfors, A., Jager, E.W.H.: Mechanical stimulation of epithelial cells using polypyrrole microactuators. *Lab Chip* **11**, 3287 (2011). <https://doi.org/10.1039/c1lc20436j>
51. Wan, C., Chung, S., Kamm, R.D.: Differentiation of embryonic stem cells into cardiomyocytes in a compliant microfluidic system. *Ann. Biomed. Eng.* **39**, 1840–1847 (2011). <https://doi.org/10.1007/s10439-011-0275-8>
52. Zheng, W., Jiang, B., Wang, D., Zhang, W., Wang, Z., Jiang, X.: A microfluidic flow-stretch chip for investigating blood vessel biomechanics. *Lab Chip* **12**, 3441 (2012). <https://doi.org/10.1039/c2lc40173h>
53. Huh, D., Matthews, B.D., Mammoto, A., Montoya-Zavala, M., Hsin, H.Y., Ingber, D.E.: Reconstituting organ-level lung functions on a chip. *Science* **1979**(328), 1662–1668 (2010). <https://doi.org/10.1126/science.1188302>
54. Sung, J.H., Yu, J., Luo, D., Shuler, M.L., March, J.C.: Microscale 3-D hydrogel scaffold for biomimetic gastrointestinal (GI) tract model. *Lab Chip* **11**, 389–392 (2011). <https://doi.org/10.1039/C0LC00273A>
55. Taylor, A.M., Rhee, S.W., Tu, C.H., Cribbs, D.H., Cotman, C.W., Jeon, N.L.: Microfluidic multi-compartment device for neuroscience research. *Langmuir* **19**, 1551–1556 (2003). <https://doi.org/10.1021/la026417v>
56. Irimia, D., Toner, M.: Spontaneous migration of cancer cells under conditions of mechanical confinement. *Integr. Biol.* **1**, 506 (2009). <https://doi.org/10.1039/b908595e>
57. Ilina, O., Bakker, G.-J., Vasaturo, A., Hoffman, R.M., Friedl, P.: Two-photon laser-generated microtracks in 3D collagen lattices: principles of MMP-dependent and -independent collective cancer cell invasion. *Phys. Biol.* **8**, 029501–029501 (2011). <https://doi.org/10.1088/1478-3975/8/2/029501>
58. Lin, X., Helmke, B.P.: Micropatterned structural control suppresses mechanotaxis of endothelial cells. *Biophys. J.* **95**, 3066–3078 (2008). <https://doi.org/10.1529/biophysj.107.127761>
59. Magdesian, M.H., Sanchez, F.S., Lopez, M., Thostrup, P., Durisic, N., Belkaid, W., Liazoghli, D., Grütter, P., Colman, D.R.: Atomic force microscopy reveals important differences in axonal resistance to injury. *Biophys. J.* **103**, 405–414 (2012). <https://doi.org/10.1016/j.bpj.2012.07.003>
60. Sundararaghavan, H.G., Monteiro, G.A., Firestein, B.L., Shreiber, D.I.: Neurite growth in 3D collagen gels with gradients of mechanical properties. *Biotechnol. Bioeng.* **102**, 632–643 (2009). <https://doi.org/10.1002/bit.22074>
61. Sakar, M.S., Neal, D., Boudou, T., Borochin, M.A., Li, Y., Weiss, R., Kamm, R.D., Chen, C.S., Asada, H.H.: Formation and optogenetic control of engineered 3D skeletal muscle bioactuators. *Lab Chip* **12**, 4976–4985 (2012). <https://doi.org/10.1039/c2lc40338b>



62. Tanaka, Y., Sato, K., Shimizu, T., Yamato, M., Okano, T., Kitamori, T.: A micro-spherical heart pump powered by cultured cardiomyocytes. *Lab Chip* **7**, 207–212 (2007). <https://doi.org/10.1039/B612082B>
63. Wang, J., Heo, J., Hua, S.Z.: Spatially resolved shear distribution in microfluidic chip for studying force transduction mechanisms in cells. *Lab Chip* **10**, 235–239 (2010). <https://doi.org/10.1039/B914874D>
64. Rossi, M., Lindken, R., Hierck, B.P., Westerweel, J.: Tapered microfluidic chip for the study of biochemical and mechanical response at subcellular level of endothelial cells to shear flow. *Lab Chip* **9**, 1403–1411 (2009). <https://doi.org/10.1039/b822270n>
65. Price, G.M., Wong, K.H.K., Truslow, J.G., Leung, A.D., Acharya, C., Tien, J.: Effect of mechanical factors on the function of engineered human blood microvessels in microfluidic collagen gels. *Biomaterials* **31**, 6182–6189 (2010). <https://doi.org/10.1016/j.biomaterials.2010.04.041>
66. Zhou, J., Niklason, L.E.: Microfluidic artificial “vessels” for dynamic mechanical stimulation of mesenchymal stem cells. *Integr. Biol.* **4**, 1487–1497 (2012). <https://doi.org/10.1039/c2ib00171c>
67. van der Meer, A.D., Poot, A.A., Feijen, J., Vermes, I.: Analyzing shear stress-induced alignment of actin filaments in endothelial cells with a microfluidic assay. *Biomicrofluidics* **4**, 011103 (2010). <https://doi.org/10.1063/1.3366720>
68. Polacheck, W.J., Charest, J.L., Kamm, R.D.: Interstitial flow influences direction of tumor cell migration through competing mechanisms. *Proc. Natl. Acad. Sci. U.S.A.* **108**, 11115–11120 (2011). <https://doi.org/10.1073/pnas.1103581108>
69. Legant, W.R., Pathak, A., Yang, M.T., Deshpande, V.S., McMeeking, R.M., Chen, C.S.: Microfabricated tissue gauges to measure and manipulate forces from 3D microtissues. *Proc. Natl. Acad. Sci. U.S.A.* **106**, 10097–10102 (2009). <https://doi.org/10.1073/pnas.0900174106>
70. Kim, H.J., Huh, D., Hamilton, G., Ingber, D.E.: Human gut-on-a-chip inhabited by microbial flora that experiences intestinal peristalsis-like motions and flow. *Lab Chip* **12**, 2165 (2012). <https://doi.org/10.1039/c2lc40074j>
71. Mainardi, A., Cambria, E., Occhetta, P., Martin, I., Barbero, A., Schären, S., Mehrkens, A., Krupkova, O.: Intervertebral disc-on-a-chip as advanced in vitro model for mechanobiology research and drug testing: a review and perspective. *Front. Bioeng. Biotechnol.* (2022). <https://doi.org/10.3389/fbioe.2021.826867>
72. Urban, J.P.G., Smith, S., Fairbank, J.C.T.: Nutrition of the intervertebral disc. *Spine (Phila. PA 1976)* **29**, 2700–2709 (2004). <https://doi.org/10.1097/01.brs.0000146499.97948.52>
73. Chan, S.C.W., Ferguson, S.J., Gantenbein-Ritter, B.: The effects of dynamic loading on the intervertebral disc. *Eur. Spine J.* **20**, 1796–1812 (2011). <https://doi.org/10.1007/s00586-011-1827-1>
74. Wuertz, K., Haglund, L.: Inflammatory mediators in intervertebral disk degeneration and discogenic pain. *Global Spine J.* **3**, 175–184 (2013). <https://doi.org/10.1055/s-0033-1347299>
75. Sadowska, A., Kameda, T., Krupkova, O., Wuertz-Kozak, K.: Osmosensing, osmosignalling and inflammation: how intervertebral disc cells respond to altered osmolarity. *Eur. Cell. Mater.* **36**, 231–250 (2018). <https://doi.org/10.22203/eCM.v036a17>
76. Dai, J., Xing, Y., Xiao, L., Li, J., Cao, R., He, Y., Fang, H., Periasamy, A., Oberholzner, J., Jin, L., Landers, J.P., Wang, Y., Li, X.: Microfluidic disc-on-a-chip device for mouse intervertebral disc—pitching a next-generation research platform to study disc degeneration. *ACS Biomater. Sci. Eng.* **5**, 2041–2051 (2019). <https://doi.org/10.1021/acsbiomaterials.8b01522>
77. Chou, P.-H., Wang, S.-T., Yen, M.-H., Liu, C.-L., Chang, M.-C., Lee, O.K.-S.: Fluid-induced, shear stress-regulated extracellular matrix and matrix metalloproteinase genes expression on human annulus fibrosus cells. *Stem Cell Res. Ther.* **7**, 34 (2016). <https://doi.org/10.1186/s13287-016-0292-5>
78. Sivaraman, A., Leach, J., Townsend, S., Iida, T., Hogan, B., Stolz, D., Fry, R., Samson, L., Tannenbaum, S., Griffith, L.: A microscale in vitro physiological model of the liver: predictive screens for drug metabolism and enzyme induction. *Curr. Drug Metab.* **6**, 569–591 (2005). <https://doi.org/10.2174/138920005774832632>
79. Liegibel, U., Sommer, U., Bundschuh, B., Schweizer, B., Hilscher, U., Lieder, A., Nawroth, P., Kasperk, C.: Fluid shear of low magnitude increases growth and expression of TGFβ1 and adhesion molecules in human bone cells in vitro. *Exp. Clin. Endocrinol. Diabetes* **112**, 356–363 (2004). <https://doi.org/10.1055/s-2004-821014>
80. Boccazzi, P., Zanzotto, A., Szita, N., Bhattacharya, S., Jensen, K.F., Sinskey, A.J.: Gene expression analysis of *Escherichia coli* grown in miniaturized bioreactor platforms for high-throughput analysis of growth and genomic data. *Appl. Microbiol. Biotechnol.* **68**, 518–532 (2005). <https://doi.org/10.1007/s00253-005-1966-6>
81. Vilkner, T., Janasek, D., Manz, A.: Micro total analysis systems. Recent developments. *Anal. Chem.* **76**, 3373–3386 (2004). <https://doi.org/10.1021/ac040063q>

82. Lion, N., Rohner, T.C., Dayon, L., Arnaud, I.L., Damoc, E., Youhnovski, N., Wu, Z.-Y., Roussel, C., Jossierand, J., Jensen, H., Rossier, J.S., Przybylski, M., Girault, H.H.: Microfluidic systems in proteomics. *Electrophoresis* **24**, 3533–3562 (2003). <https://doi.org/10.1002/elps.200305629>
83. Aurox, P.-A., Koc, Y., deMello, A., Manz, A., Day, P.J.R.: Miniaturised nucleic acid analysis. *Lab Chip* **4**, 534–546 (2004). <https://doi.org/10.1039/b408850f>
84. Andersson, H., van den Berg, A.: Microfluidic devices for cellomics: a review. *Sens. Actuators B Chem.* **92**, 315–325 (2003). [https://doi.org/10.1016/S0925-4005\(03\)00266-1](https://doi.org/10.1016/S0925-4005(03)00266-1)
85. Verpoorte, E.: Microfluidic chips for clinical and forensic analysis. *Electrophoresis* **23**, 677–712 (2002). [https://doi.org/10.1002/1522-2683\(200203\)23:5%3c677::AID-ELPS677%3e3.0.CO;2-8](https://doi.org/10.1002/1522-2683(200203)23:5%3c677::AID-ELPS677%3e3.0.CO;2-8)
86. Breslauer, D.N., Lee, P.J., Lee, L.P.: Microfluidics-based systems biology. *Mol. Biosyst.* **2**, 97–112 (2006). <https://doi.org/10.1039/b515632g>
87. Bertani, G., Di Tinco, R., Bertoni, L., Orlandi, G., Pisciotta, A., Rosa, R., Rigamonti, L., Signore, M., Bertacchini, J., Sena, P., De Biasi, S., Villa, E., Carnevale, G.: Flow-dependent shear stress affects the biological properties of pericyte-like cells isolated from human dental pulp. *Stem Cell Res. Ther.* **14**, 31 (2023). <https://doi.org/10.1186/s13287-023-03254-2>
88. Li Jeon, N., Baskaran, H., Dertinger, S.K.W., Whitesides, G.M., Van De Water, L., Toner, M.: Neutrophil chemotaxis in linear and complex gradients of interleukin-8 formed in a microfabricated device. *Nat. Biotechnol.* **20**, 826–830 (2002). <https://doi.org/10.1038/nbt712>
89. Hung, P.J., Lee, P.J., Sabounchi, P., Lin, R., Lee, L.P.: Continuous perfusion microfluidic cell culture array for high-throughput cell-based assays. *Biotechnol. Bioeng.* **89**, 1–8 (2005). <https://doi.org/10.1002/bit.20289>
90. Yang, M., Li, C.-W., Yang, J.: Cell docking and on-chip monitoring of cellular reactions with a controlled concentration gradient on a microfluidic device. *Anal. Chem.* **74**, 3991–4001 (2002). <https://doi.org/10.1021/ac025536c>
91. El-Ali, J., Gaudet, S., Günther, A., Sorger, P.K., Jensen, K.F.: Cell stimulus and lysis in a microfluidic device with segmented gas–liquid flow. *Anal. Chem.* **77**, 3629–3636 (2005). <https://doi.org/10.1021/ac050008x>
92. Hu, X., Arnold, W.M., Zimmermann, U.: Alterations in the electrical properties of T and B lymphocyte membranes induced by mitogenic stimulation. Activation monitored by electro-rotation of single cells. *Biochim. Biophys. Acta Biomembr.* **1021**, 191–200 (1990). [https://doi.org/10.1016/0005-2736\(90\)90033-K](https://doi.org/10.1016/0005-2736(90)90033-K)
93. Hu, X., Bessette, P.H., Qian, J., Meinhart, C.D., Daugherty, P.S., Soh, H.T.: Marker-specific sorting of rare cells using dielectrophoresis. *Proc. Natl. Acad. Sci. U.S.A.* **102**, 15757–15761 (2005). <https://doi.org/10.1073/pnas.0507719102>
94. Li, P.C.H., Harrison, D.J.: Transport, manipulation, and reaction of biological cells on-chip using electrokinetic effects. *Anal. Chem.* **69**, 1564–1568 (1997). <https://doi.org/10.1021/ac9606564>
95. Lee, S.-W., Tai, Y.-C.: A micro cell lysis device. *Sens. Actuators A Phys.* **73**, 74–79 (1999). [https://doi.org/10.1016/S0924-4247\(98\)00257-X](https://doi.org/10.1016/S0924-4247(98)00257-X)
96. Lu, H., Schmidt, M.A., Jensen, K.F.: A microfluidic electroporation device for cell lysis. *Lab Chip* **5**, 23–29 (2005). <https://doi.org/10.1039/b406205a>
97. Jeon, H., Kim, S., Lim, G.: Electrical force-based continuous cell lysis and sample separation techniques for development of integrated microfluidic cell analysis system: A review. *Microelectron. Eng.* **198**, 55–72 (2018). <https://doi.org/10.1016/j.mee.2018.06.010>
98. Huang, Y., Agrawal, B., Sun, D., Kuo, J.S., Williams, J.C.: Microfluidics-based devices: new tools for studying cancer and cancer stem cell migration. *Biomicrofluidics* **5**, 013412 (2011). <https://doi.org/10.1063/1.3555195>
99. Suresh, S.: Biomechanics and biophysics of cancer cells. *Acta Biomater.* **3**, 413–438 (2007). <https://doi.org/10.1016/j.actbio.2007.04.002>
100. Hou, H.W., Li, Q.S., Lee, G.Y.H., Kumar, A.P., Ong, C.N., Lim, C.T.: Deformability study of breast cancer cells using microfluidics. *Biomed. Microdevices* **11**, 557–564 (2009). <https://doi.org/10.1007/s10544-008-9262-8>
101. Hur, S.C., Henderson-MacLennan, N.K., McCabe, E.R.B., Di Carlo, D.: Deformability-based cell classification and enrichment using inertial microfluidics. *Lab Chip* **11**, 912–920 (2011). <https://doi.org/10.1039/c0lc00595a>
102. Walker, G.M., Sai, J., Richmond, A., Stremler, M., Chung, C.Y., Wikswo, J.P.: Effects of flow and diffusion on chemotaxis studies in a microfabricated gradient generator. *Lab Chip* **5**, 611–618 (2005). <https://doi.org/10.1039/b417245k>
103. Cheung, L.S.L., Zheng, X., Stopa, A., Baygents, J.C., Guzman, R., Schroeder, J.A., Heimark, R.L., Zohar, Y.: Detachment of captured cancer cells under flow acceleration in a bio-functionalized microchannel. *Lab Chip* **9**, 1721–1731 (2009). <https://doi.org/10.1039/b822172c>

104. Li, J., Lin, F.: Microfluidic devices for studying chemotaxis and electrotaxis. *Trends Cell Biol.* **21**, 489–497 (2011). <https://doi.org/10.1016/j.tcb.2011.05.002>
105. Tanaka, T., Ishikawa, T., Numayama-Tsuruta, K., Imai, Y., Ueno, H., Yoshimoto, T., Matsuki, N., Yamaguchi, T.: Inertial migration of cancer cells in blood flow in microchannels. *Biomed. Micro-devices* **14**, 25–33 (2012). <https://doi.org/10.1007/s10544-011-9582-y>
106. Migita, S., Funakoshi, K., Tsuya, D., Yamazaki, T., Taniguchi, A., Sugimoto, Y., Hanagata, N., Ikoma, T.: Cell cycle and size sorting of mammalian cells using a microfluidic device. *Anal. Methods* **2**, 657–660 (2010). <https://doi.org/10.1039/c0ay00039f>
107. Choi, S., Song, S., Choi, C., Park, J.-K.: Microfluidic self-sorting of mammalian cells to achieve cell cycle synchrony by hydrophoresis. *Anal. Chem.* **81**, 1964–1968 (2009). <https://doi.org/10.1021/ac8024575>
108. Thévoz, P., Adams, J.D., Shea, H., Bruus, H., Soh, H.T.: Acoustophoretic synchronization of mammalian cells in microchannels. *Anal. Chem.* **82**, 3094–3098 (2010). <https://doi.org/10.1021/ac100357u>
109. Zborowski, M., Chalmers, J.J.: Rare cell separation and analysis by magnetic sorting. *Anal. Chem.* **83**, 8050–8056 (2011). <https://doi.org/10.1021/ac200550d>
110. Plouffe, B.D., Mahalanabis, M., Lewis, L.H., Klapperich, C.M., Murthy, S.K.: Clinically relevant microfluidic magnetophoretic isolation of rare-cell populations for diagnostic and therapeutic monitoring applications. *Anal. Chem.* **84**, 1336–1344 (2012). <https://doi.org/10.1021/ac2022844>
111. Liu, Y.-J., Guo, S.-S., Zhang, Z.-L., Huang, W.-H., Baigl, D., Xie, M., Chen, Y., Pang, D.-W.: A micropillar-integrated smart microfluidic device for specific capture and sorting of cells. *Electrophoresis* **28**, 4713–4722 (2007). <https://doi.org/10.1002/elps.200700212>
112. Saliba, A.-E., Saia, S., Psychari, E., Minc, N., Simon, D., Bidard, F.-C., Mathiot, C., Pierga, J.-Y., Fraiser, V., Salamero, J., Saada, V., Farace, F., Vielh, P., Malaquin, L., Viovy, J.-L.: Microfluidic sorting and multimodal typing of cancer cells in self-assembled magnetic arrays. *Proc. Natl. Acad. Sci. U.S.A.* **107**, 14524–14529 (2010). <https://doi.org/10.1073/pnas.1001515107>
113. Adams, J.D., Kim, U., Soh, H.T.: Multitarget magnetic activated cell sorter. *Proc. Natl. Acad. Sci. U.S.A.* **105**, 18165–18170 (2008). <https://doi.org/10.1073/pnas.0809795105>
114. Shen, F., Hwang, H., Hahn, Y.K., Park, J.-K.: Label-free cell separation using a tunable magnetophoretic repulsion force. *Anal. Chem.* **84**, 3075–3081 (2012). <https://doi.org/10.1021/ac201505j>
115. Fu, A.Y., Spence, C., Scherer, A., Arnold, F.H., Quake, S.R.: A microfabricated fluorescence-activated cell sorter. *Nat. Biotechnol.* **17**, 1109–1111 (1999). <https://doi.org/10.1038/15095>
116. Inglis, D.W., Davis, J.A., Zieziulewicz, T.J., Lawrence, D.A., Austin, R.H., Sturm, J.C.: Determining blood cell size using microfluidic hydrodynamics. *J. Immunol. Methods* **329**, 151–156 (2008). <https://doi.org/10.1016/j.jim.2007.10.004>
117. Kim, U., Qian, J., Kenrick, S.A., Daugherty, P.S., Soh, H.T.: Multitarget dielectrophoresis activated cell sorter. *Anal. Chem.* **80**, 8656–8661 (2008). <https://doi.org/10.1021/ac8015938>
118. Kim, U., Soh, H.T.: Simultaneous sorting of multiple bacterial targets using integrated dielectrophoretic-magnetic activated cell sorter. *Lab Chip* **9**, 2313–2318 (2009). <https://doi.org/10.1039/b903950c>
119. Cho, S.H., Chen, C.H., Tsai, F.S., Godin, J.M., Lo, Y.-H.: Human mammalian cell sorting using a highly integrated micro-fabricated fluorescence-activated cell sorter ( $\mu$ FACS). *Lab Chip* **10**, 1567–1573 (2010). <https://doi.org/10.1039/c000136h>
120. An, J., Lee, J., Lee, S.H., Park, J., Kim, B.: Separation of malignant human breast cancer epithelial cells from healthy epithelial cells using an advanced dielectrophoresis-activated cell sorter (DACS). *Anal. Bioanal. Chem.* **394**, 801–809 (2009). <https://doi.org/10.1007/s00216-009-2743-7>
121. Lau, A.Y., Lee, L.P., Chan, J.W.: An integrated optofluidic platform for Raman-activated cell sorting. *Lab Chip* **8**, 1116–1120 (2008). <https://doi.org/10.1039/b803598a>
122. Jang, K.-J., Suh, K.-Y.: A multi-layer microfluidic device for efficient culture and analysis of renal tubular cells. *Lab Chip* **10**, 36–42 (2010). <https://doi.org/10.1039/B907515A>

**Publisher's Note** Springer Nature remains neutral with regard to jurisdictional claims in published maps and institutional affiliations.

Springer Nature or its licensor (e.g. a society or other partner) holds exclusive rights to this article under a publishing agreement with the author(s) or other rightsholder(s); author self-archiving of the accepted manuscript version of this article is solely governed by the terms of such publishing agreement and applicable law.